NANO LETTERS
Cite This: Nano Lett. 2019, 19, 7400−7410
Letter
pubs.acs.org/NanoLett

Mechanostability of the Fibrinogen Bridge between Staphylococcal Surface Protein ClfA and Endothelial Cell Integrin $\alpha_V\beta_3$

Felipe Viela,[†] Pietro Speziale,[‡,§] Giampiero Pietrocola,[*,‡] and Yves F. Dufrêne[*,†,∥]

[†]Louvain Institute of Biomolecular Science and Technology, UCLouvain, Croix du Sud, 4-5, bte L7.07.06, B-1348 Louvain-la-Neuve, Belgium

[‡]Department of Molecular Medicine, Unit of Biochemistry, University of Pavia, Viale Taramelli 3/b, 27100 Pavia, Italy

[§]Department of Industrial and Information Engineering, University of Pavia, 27100 Pavia, Italy

[∥]Walloon Excellence in Life sciences and Biotechnology (WELBIO), 1300 Wavre, Belgium

ABSTRACT: Binding of the *Staphylococcus aureus* surface protein clumping factor A (ClfA) to endothelial cell integrin $\alpha_V\beta_3$ plays a crucial role during sepsis, by causing endothelial cell apoptosis and loss of barrier integrity. ClfA uses the blood plasma protein fibrinogen (Fg) to bind to $\alpha_V\beta_3$ but how this is achieved at the molecular level is not known. Here we investigate the mechanical strength of the three-component ClfA-Fg-$\alpha_V\beta_3$ interaction on living bacteria, by means of single-molecule experiments. We find that the ClfA-Fg-$\alpha_V\beta_3$ ternary complex is extremely stable, being able to sustain forces (~800 pN) that are much stronger than those of classical bonds between integrins and the Arg-Gly-Asp (RGD) tripeptide sequence (~100 pN). Adhesion forces between single bacteria and $\alpha_V\beta_3$ are strongly inhibited by an anti-$\alpha_V\beta_3$ antibody, the RGD peptide, and the cyclic RGD peptide cilengitide, showing that formation of the complex involves RGD-dependent binding sites and can be efficiently inhibited by $\alpha_V\beta_3$ blockers. Collectively, our experiments favor a binding mechanism involving the extraordinary elasticity of Fg. In the absence of mechanical stress, $RGD^{572-574}$ sequences in the Aα chains mediate weak binding to $\alpha_V\beta_3$, whereas under high mechanical stress exposure of cryptic Aα chain RGD^{95-97} sequences leads to extremely strong binding to the integrin. Our results identify an unexpected and previously undescribed force-dependent binding mechanism between ClfA and $\alpha_V\beta_3$ on endothelial cells, which could represent a potential target to fight staphylococcal bloodstream infections.

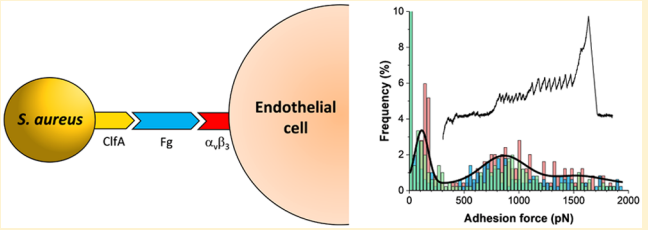

KEYWORDS: *Staphylococcus aureus, sepsis, protein clumping factor A, integrin $\alpha_V\beta_3$, fibrinogen bridge, single-molecule experiments, AFM*

Staphylococcus aureus is a Gram-positive bacterial pathogen that causes a variety of infections, ranging from mild skin diseases, such as impetigo and cellulitis[1,2] to serious invasive diseases like bloodstream infection.[3] Sepsis is the body's overwhelming and life-threatening response to infection that can lead to tissue damage and organ dysfunction culminating in death.[4] The endothelium is a major target of sepsis condition and endothelial damage accounts for much of the pathology. *S. aureus* has developed sophisticated mechanisms to attach to endothelial cells lining the heart and vessel wall and to the exposed subendothelial matrix. Among the multitude of *S. aureus* virulence factors, cell wall-anchored (CWA) proteins such as fibronectin-binding proteins FnBPA/B and clumping factor A (ClfA) mediate adhesion to host cells and to extracellular matrix components.[5] ClfA is a fibrinogen (Fg)-binding protein that plays a dual role in *S. aureus*-endothelium adhesion, that is, via von Willebrand factor binding protein (vWFbp)-dependent attachment to endothelial VWF under shear stress,[6] and binding to endothelial cell $\alpha_V\beta_3$ integrin in the presence of Fg. Attachment of *S. aureus* to vascular endothelial cells results in Ca^{2+} mobilization, exocytosis of granules and deposition of vWF on the surface of endothelial cells (Figure 1A). In turn, a significant disturbance in barrier integrity occurs due to the reduction in VE-cadherin expression in the cell membrane. The macroscopic consequences of these biological events include cell−cell detachment, increased vascular permeability, and ultimately cell death by apoptosis. ClfA binding to $\alpha_V\beta_3$ is significantly inhibited by cilengitide (Figure 1A) and prevents endothelial dysfunction, suggesting that the integrin is a potential target to treat *S. aureus* bloodstream infections.[7]

S. aureus adhesion to vascular endothelial cells involves the formation of the ClfA-Fg-$\alpha_V\beta_3$ ternary complex and thus of ClfA-Fg and Fg-$\alpha_V\beta_3$ bonds. ClfA binds the carboxy-terminus of the γ-chain of Fg through a variation of the multistep "dock, lock, and latch" (DLL) mechanism[8] first described for the binding of the *S. epidermidis* protein SdrG to Fg.[9] The N-terminus of ClfA contains a signal sequence followed by the ligand-binding region A composed of three separately folded

Received: July 27, 2019
Revised: September 3, 2019
Published: September 18, 2019

DOI: 10.1021/acs.nanolett.9b03080
Nano Lett. 2019, 19, 7400−7410

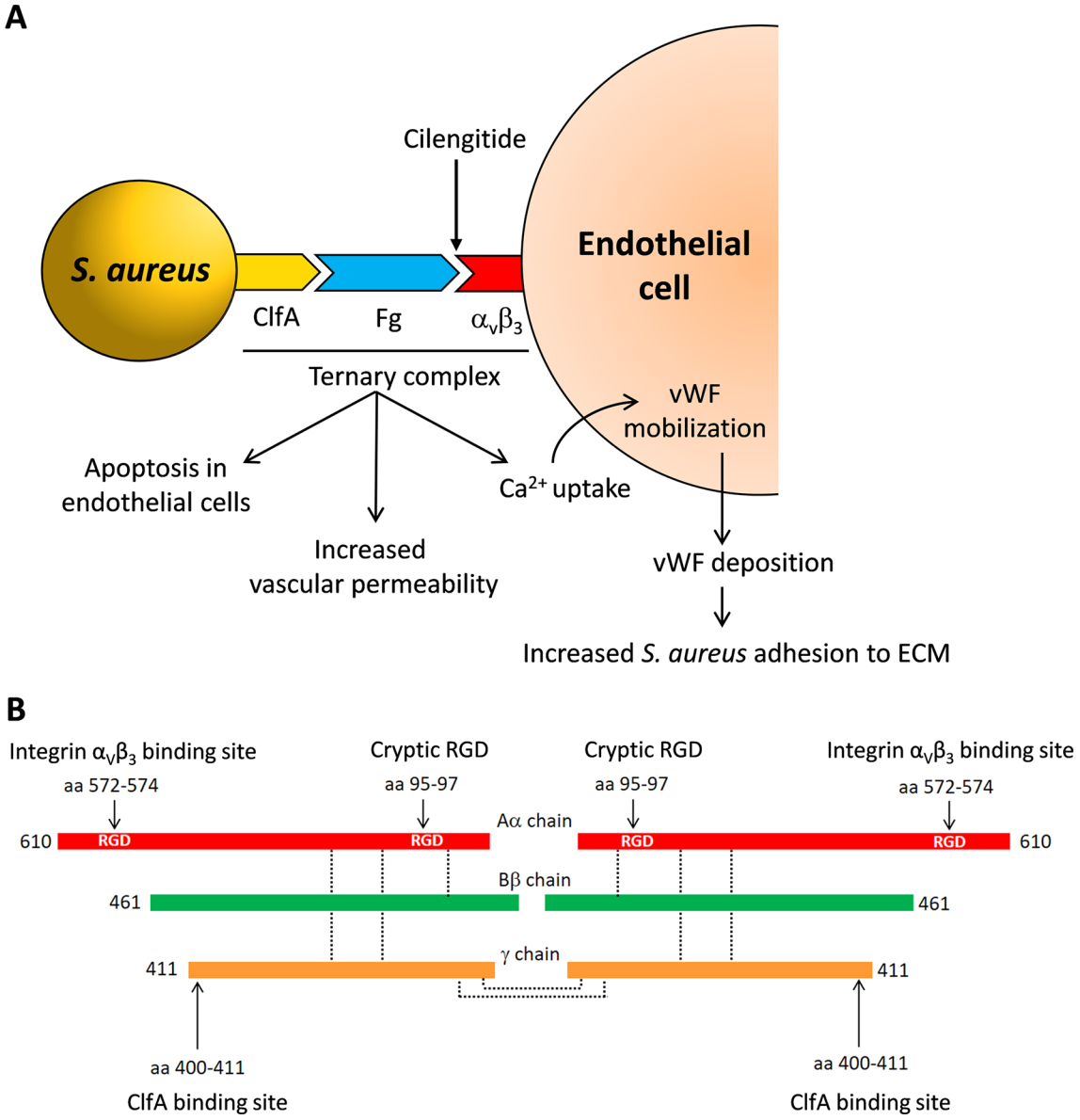

Figure 1. Biological significance of the Fg-dependent bridge between ClfA on the bacterial surface and $\alpha_V\beta_3$ in the host cell membrane. (A) During sepsis, attachment of *S. aureus* surface protein ClfA to endothelial cell integrin $\alpha_V\beta_3$ induces endothelial cell apoptosis and loss of barrier integrity. ClfA uses the blood protein Fg to bridge $\alpha_V\beta_3$ under shear stress conditions. Cilengitide is a cyclic Arg-Gly-Asp (RGD)-derived peptide binding with high affinity to $\alpha_V\beta_3$. (B) Schematic structure of Fg, emphasizing ClfA and RGD-dependent $\alpha_V\beta_3$ binding sites, as well as RGD cryptic sequences.

domains N1, N2, and N3. The carboxy-terminus of the γ-chain docks in a ligand-binding trench located between domains N2 and N3. The DLL mechanism involves dynamic conformational changes of the adhesin that result in a greatly stabilized adhesin-ligand complex with a strength equivalent to that of a covalent bond.[10,11] The overall affinity of Fg binding is increased through interaction with a recently described second site that lies at the top of subdomain N3 outside of the DLL ligand-binding trench.[12]

As all integrins, $\alpha_V\beta_3$ is a heterodimer of noncovalently associated α- and β-subunits, expressed at the surface of mammalian cells.[13,14] The α- and β-subunits are composed of several domains with flexible linkers between them. Each subunits has a single membrane-spanning helix and, usually, a short cytoplasmic tail. $\alpha_V\beta_3$ is the major integrin expressed on the surface of endothelial cells and is involved in tumor angiogenesis, metastasis, inflammation, and bone resorption.[15] It binds to multiple ligands including vitronectin, fibronectin, vWF, and Fg and also serves as a receptor for several viruses such as adenovirus and human immunodeficient virus.[16] $\alpha_V\beta_3$ shares with other integrins the ability to recognize the Arg-Gly-Asp (RGD) tripeptide sequence found in several extracellular matrix (ECM) proteins, such as Fg, thereby promoting cell adhesion to the ECM. RGD binds at the interface between the α- and β-subunits with variable affinity, possibly reflecting differences in the fitting of the ligand RGD conformation with the specific $\alpha-\beta$ active site pocket.[17] Fg-binding by $\alpha_V\beta_3$ involves a RGD sequence at Aα chain residues 572−574[18] (Figure 1B). Another RGD sequence at Aα chain residues 95−97 fails to bind in standard bioassays.[19] In addition, two γ chain-derived peptides GWTVFQKRLDGSV$^{190-202}$ and GVYYQGGTYSKAS$^{346-358}$ were shown to block $\alpha_V\beta_3$-

DOI: 10.1021/acs.nanolett.9b03080
Nano Lett. 2019, 19, 7400−7410

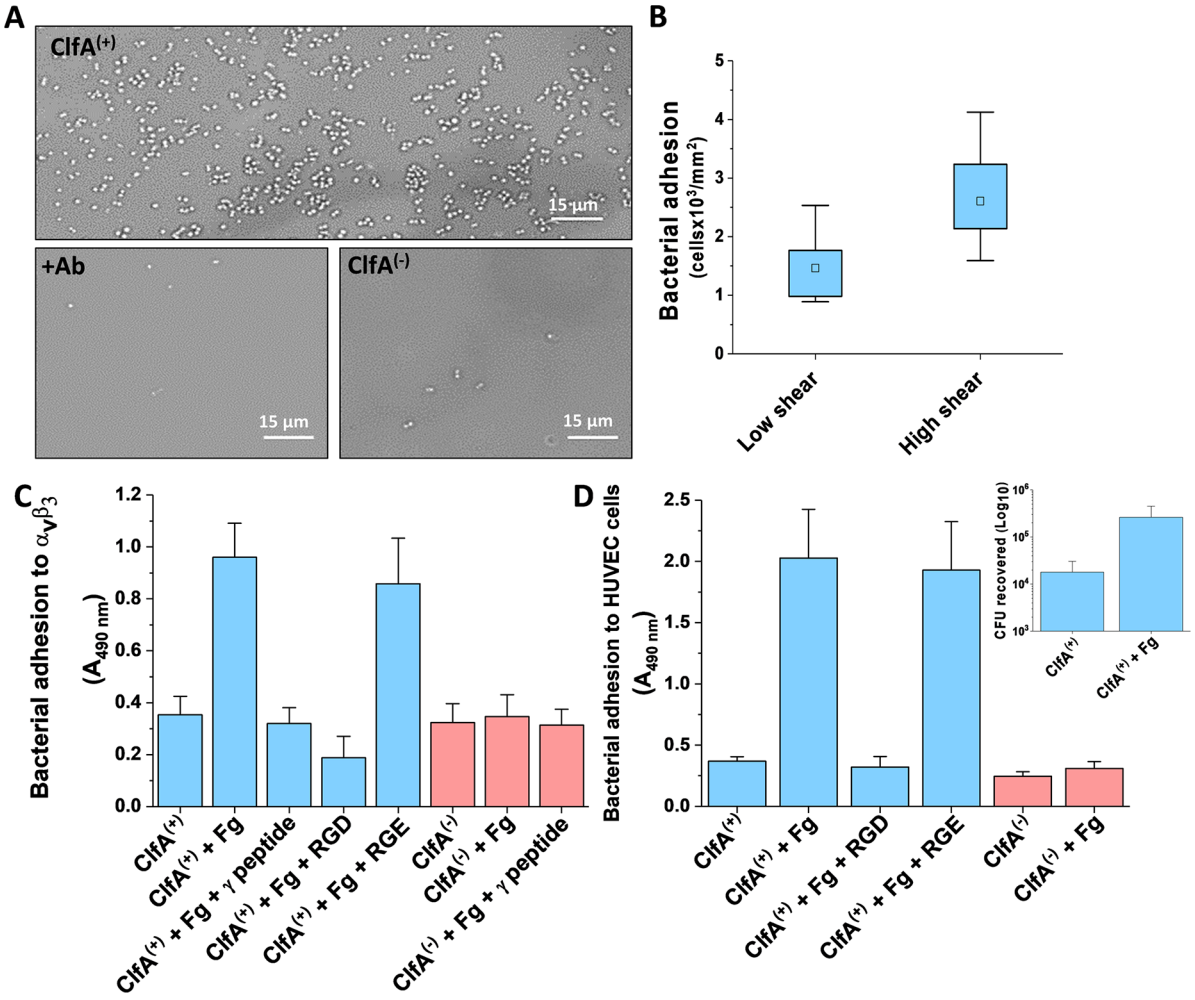

Figure 2. Role of the ClfA-Fg-$\alpha_V\beta_3$ interaction in *S. aureus* adhesion. (A) Optical microscopy images of bacteria adhering to $\alpha_V\beta_3$-coated substrates: Fg-pretreated ClfA$^{(+)}$ cells, Fg-pretreated ClfA$^{(+)}$ cells incubated with $\alpha_V\beta_3$ surfaces blocked with LM 609 antibody, and Fg-pretreated ClfA$^{(-)}$ cells. (B) Quantification of Fg-pretreated ClfA$^{(+)}$ cells adhering to $\alpha_V\beta_3$-coated substrates in a flow chamber under low and high shear stresses. Boxplots represent the mean values (squares), 25 and 75% quartiles (box plot limits) and outliers (whiskers) from 10 images from 2 different experiments. (C) Bacterial attachment to microtiter wells coated with $\alpha_v\beta_3$. Coated wells were mixed with/without Fg and incubated with *S. aureus* ClfA$^{(+)}$ or ClfA$^{(-)}$ cells. After washing, attached bacteria were detected by mouse HRP-conjugated antibody. Where indicated, integrin-coated wells were incubated with Fg in the presence/absence of the synthetic dodecapeptide mimicking the C-terminal segment of the Fg γ chain (residues 400–411). The effect of RGD or RGE peptides on the adhesion of ClfA$^{(+)}$ to $\alpha_V\beta_3$ preincubated with Fg was also tested. Shown here are the means and standard deviation of results of three independent experiments, each performed in duplicate. (D) Bacterial adhesion to endothelial cell monolayers. Confluent HUVEC monolayers were pretreated or not with Fg and incubated with *S. aureus* ClfA$^{(+)}$ or ClfA$^{(-)}$ cells. After washing, attached bacteria were detected by addition of HRP-conjugated antibody to the wells. Where indicated, the effect of RGD or RGE peptides was tested. Alternatively (inset), confluent cell monolayers were incubated with *S. aureus* ClfA$^{(+)}$ in the presence/absence of Fg. Monolayers were extensively washed, lysed, and CFU (colony forming units) counted by serial dilution of endothelial lysates and plating onto brain heart infusion agar plates. Shown here are the means and standard deviation of results of two independent experiments, each performed in duplicate.

mediated cell adhesion. These sequences are located next to each other in the γ-chain crystal structure, although they are separated in the primary structure, suggesting the two segments are part of the $\alpha_V\beta_3$ binding site and concur to its formation.[20]

Despite the medical relevance of ClfA-mediated adhesion to vascular endothelial cells, we presently know very little about the molecular mechanism guiding the formation and stability of the ClfA-Fg-$\alpha_V\beta_3$ complex. Here single-molecule atomic force microscopy (AFM)[21] is used to investigate the mechanostability of this three-component interaction. The results show that the Fg bridge between ClfA and $\alpha_V\beta_3$ is extremely strong and point to a model where this high mechanostability results from the force-induced exposure of cryptic RGD binding sites in the Fg molecule.

Results and Discussion. *Role of the ClfA-Fg-$\alpha_V\beta_3$ Interaction in Bacterial Adhesion.* To study the ClfA-Fg-$\alpha_V\beta_3$ interaction, we used *S. aureus* SH1000 *clfA clfB fnbA fnbB* (here after called *S. aureus* ClfA$^{(-)}$ cells) and the same mutant strain transformed with a plasmid expressing the entire *clfA* gene (ClfA$^{(+)}$ cells).[22] The role of the ternary complex in bacterial adhesion was first assessed by optical microscopy. Bacteria expressing full length ClfA (ClfA$^{(+)}$) were pretreated with soluble Fg and incubated in static conditions with $\alpha_V\beta_3$-conditioned plastic substrates. Unlike bacteria lacking ClfA (ClfA$^{(-)}$), ClfA$^{(+)}$ bacteria adhered in large amounts to $\alpha_V\beta_3$ surfaces. Adhesion was abrogated when $\alpha_V\beta_3$ surfaces were

DOI: 10.1021/acs.nanolett.9b03080
Nano Lett. 2019, 19, 7400–7410

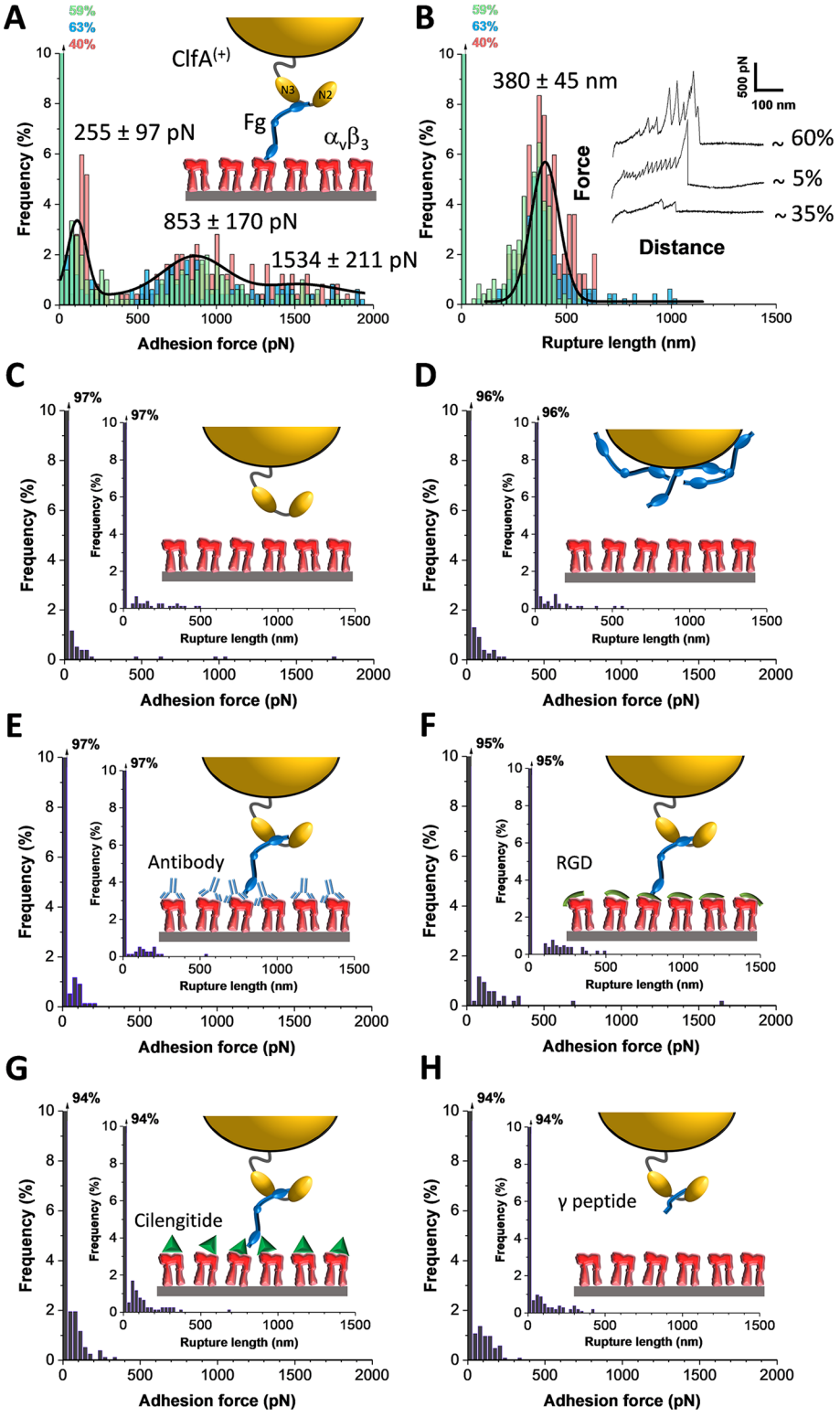

Figure 3. Fg-dependent adhesion forces between single bacteria and $\alpha_V\beta_3$ integrins. (A, B) Adhesion force and rupture length histograms with representative force profiles obtained by recording force−distance curves in PBS between *S. aureus* ClfA$^{(+)}$ cells pretreated with Fg and $\alpha_V\beta_3$ immobilized on solid substrates. (C) Force data between untreated *S. aureus* ClfA$^{(+)}$ cells and $\alpha_V\beta_3$ substrates. (D) Force data between *S. aureus* ClfA$^{(-)}$ cells pretreated with Fg and $\alpha_V\beta_3$ substrates. (E−G) Force data between Fg pretreated *S. aureus* ClfA$^{(+)}$ cells and $\alpha_V\beta_3$ substrates, following addition of anti-$\alpha_V\beta_3$ antibody LM609, RGD peptide, or cilengitide, respectively. (H) Force data between *S. aureus* ClfA$^{(+)}$ cells pretreated with the short γ-chain peptide of Fg. For each panel, data from three representative bacterial cells are shown (for more cells, see Figure 5).

incubated with the anti-integrin RGD recognition site antibody LM609[23] (Figure 2A), thus showing that ClfA specifically couples to $\alpha_V\beta_3$ integrin in the presence of Fg. As fluid shear stress favors ClfA-dependent *S. aureus* adhesion,[22] we also studied bacterial adhesion under flow using a microparallel flow chamber (Figure 2B). Adhesion of Fg-treated ClfA$^{(+)}$ cells

DOI: 10.1021/acs.nanolett.9b03080
Nano Lett. 2019, 19, 7400−7410

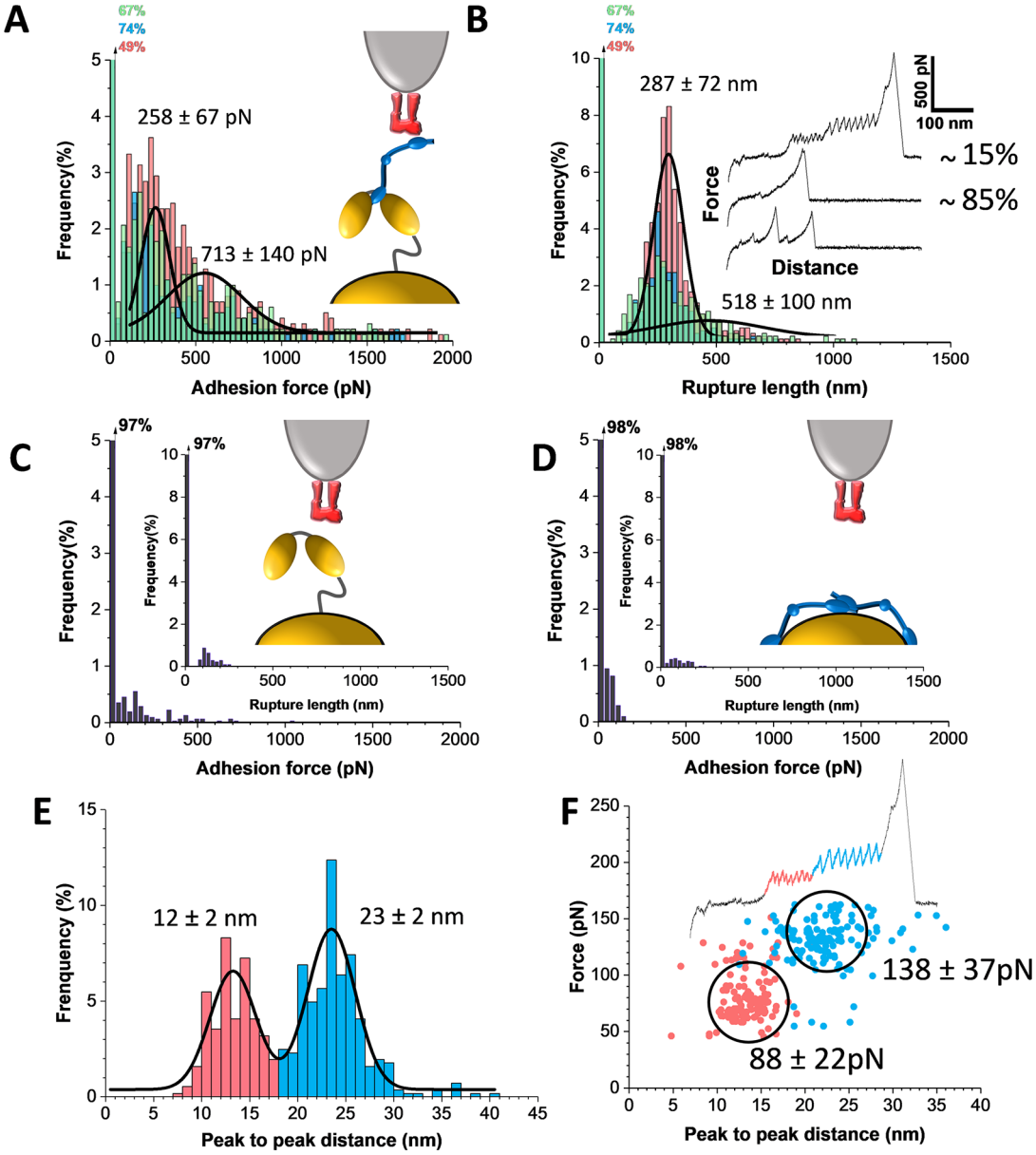

Figure 4. The Fg bridge between ClfA and $\alpha_V\beta_3$ is extremely strong. (A) Maximum adhesion force histograms and (B) rupture length histograms with representative retraction force profiles (insets) obtained by recording force−distance curves in PBS between *S. aureus* ClfA$^{(+)}$ cells pretreated with Fg and $\alpha_V\beta_3$-modified AFM tips. (C,D) Force data obtained for untreated *S. aureus* ClfA$^{(+)}$ cells (C) and for Fg-pretreated *S. aureus* ClfA$^{(-)}$ cells (D). Data from three representative bacteria are shown (for more cells, see Figure 5). (E) Distribution of peak-to-peak distances associated with Fg unfolding, documenting multiple small unfolding events of 88 ± 22 pN separated by 12 ± 2 nm, and larger events of 138 ± 37 pN separated by 23 ± 2 nm. (F) Plot of unfolding force as a function of the peak-to-peak distance, showing that low forces are associated with short distances, while high forces are linked to longer distances.

to $\alpha_V\beta_3$ surfaces was substantially enhanced when increasing the shear rate from 12 to 120 s^{-1}, corresponding to normal venous shear rates.[24] This observation indicates that physical forces associated with fluid shear favor bacterial adhesion.

Bacterial cells were then tested for their ability to attach to $\alpha_V\beta_3$-coated microtiter wells in the absence or presence of soluble Fg (Figure 2C). ClfA$^{(+)}$ cells, but not ClfA$^{(-)}$ ones, were found to largely adhere to integrin surfaces when Fg was present. To further check the specificity of adhesion, we tested the influence of the tripeptide RGD, found in numerous proteins including fibronectin and Fg.[25] While the control peptide RGE had no inhibitory effect, the RGD peptide strongly reduced the level of adherence of ClfA$^{(+)}$ cells in the presence of Fg. Previously, it has been shown that ClfA binds the C-terminal segment of the Fg γ-chain.[26,27] Consistently, adherence of Fg-mediated ClfA$^{(+)}$ staphylococci to $\alpha_V\beta_3$ was substantially inhibited by a synthetic dodecapeptide mimicking the C-terminal moiety of the Fg γ-chain (residues 400−411).

We also checked whether Fg-mediated ClfA binding to $\alpha_V\beta_3$ is critical for the attachment of *S. aureus* to endothelial cells[7] (Figure 2D). Using a standard adhesion assay of human umbilical vein endothelial cells (HUVEC) cells, ClfA$^{(+)}$ cells, unlike ClfA$^{(-)}$ ones, were found to massively adhere to endothelial cell monolayers in the presence of Fg only, confirming the role of ClfA and Fg in endothelium colonization. When ClfA$^{(+)}$ bacterial adhesion to HUVEC

DOI: 10.1021/acs.nanolett.9b03080
Nano Lett. 2019, 19, 7400−7410

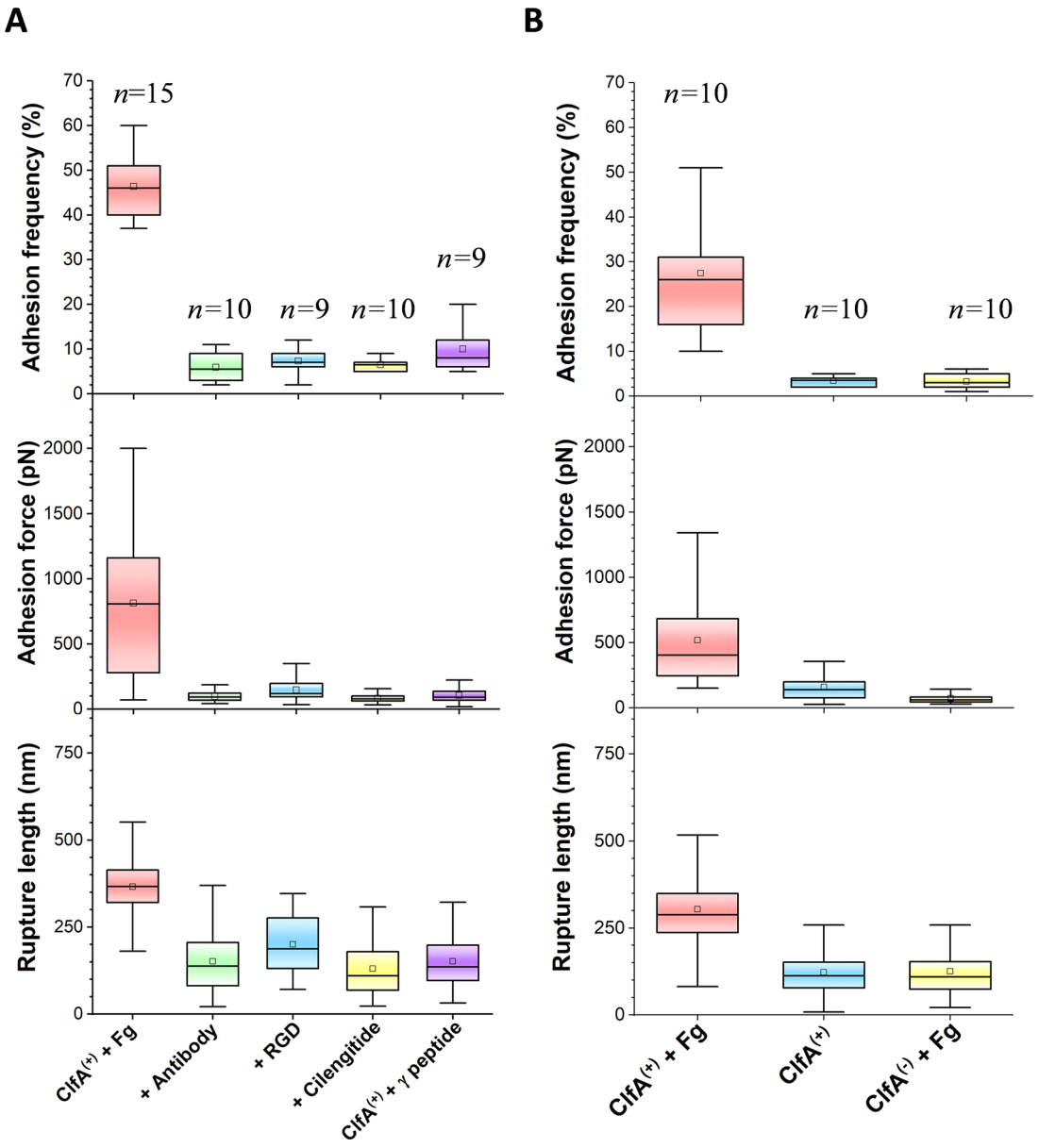

Figure 5. Strength and specificity of the ClfA-Fg-$\alpha_V\beta_3$ complex: single-cell versus single-molecule experiments. (A) Adhesion frequency, maximum adhesion force, and rupture lengths for single-cell force spectroscopy experiments obtained by probing the interaction between multiple bacteria and $\alpha_V\beta_3$ immobilized on solid substrates: Fg-pretreated ClfA$^{(+)}$ cells (n = 15 cells; 2077 adhesive curves), anti-integrin LM609 antibody (n = 10; 104 adhesive curves), RGD peptide (n = 9; 140 adhesive curves), cilengitide (n = 10; 127 adhesive curves), and Fg γ-chain peptide (n = 10; 195 adhesive curves). (B) Data from single-molecule force spectroscopy experiments obtained by probing multiple bacteria with $\alpha_V\beta_3$-modified AFM tips: Fg-pretreated ClfA$^{(+)}$ cells (n = 10; 2400 adhesive curves), native ClfA$^{(+)}$ cells (n = 10; 155 adhesive curves), and Fg-pretreated ClfA$^{(-)}$ cells (n = 10; 251 adhesive curves). Boxplots represent the mean values (squares), medians (horizontal line), 25 and 75% quartiles (box plot limits) and outliers (whiskers).

cells were detected by the CFU method (Figure 2D, inset), a significant difference between bacterial attachment in the presence and absence of Fg was observed but some residual attachment was observed in the absence of Fg, indicating that other minor adhesion mechanisms were operational. These results strongly suggest that the recombinant integrin is in its folded native conformation. Indeed, binding of bacteria to integrin-coated surfaces (Figure 2C) and attachment of *S. aureus* to endothelial cell monolayers (Figure 2D) led to very similar binding and inhibition behaviors. This shows that the conformation and activity of immobilized proteins is not substantially different from that of proteins exposed on the cell surfaces.

S. aureus Strongly Binds to $\alpha_V\beta_3$-Coated Surfaces. To study the strength of the ClfA-Fg-$\alpha_V\beta_3$ interaction, we first measured the forces between single *S. aureus* ClfA$^{(+)}$ bacteria and $\alpha_V\beta_3$ integrins immobilized on solid substrates (Figure 3). Strong adhesion was frequently detected between Fg-treated ClfA$^{(+)}$ cells and $\alpha_V\beta_3$ surfaces (adhesion frequency ~46%; mean from 3 cells) with a force distribution showing three maxima at 255 ± 97 pN, 853 ± 170 pN, and 1,534 ± 211 (mean ± s.d.; n = 542 adhesive curves from 3 cells, Figure 3A,B; for data on more cells see Figure 5A). Several lines of evidence show that these forces are primarily associated with the ClfA-Fg-$\alpha_V\beta_3$ complex. First, much weaker adhesion was measured when using native, untreated ClfA$^{(+)}$ cells (Figure

DOI: 10.1021/acs.nanolett.9b03080
Nano Lett. 2019, 19, 7400−7410

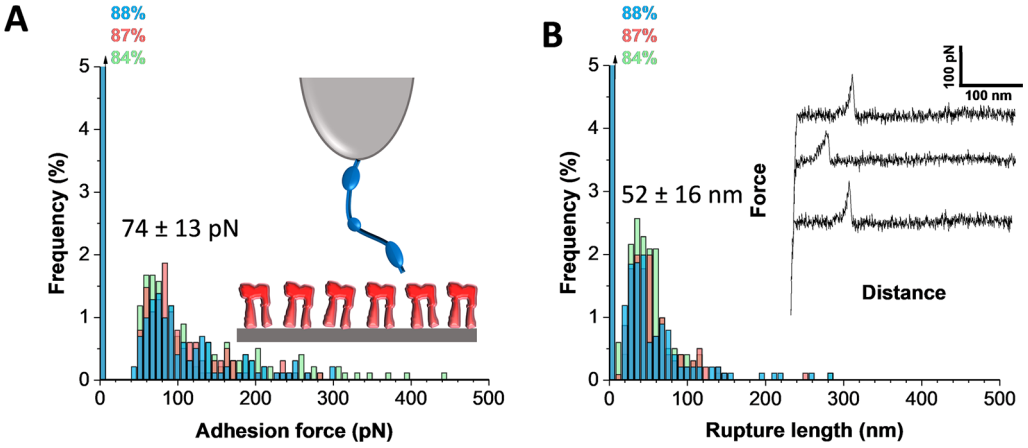

Figure 6. The bond between Fg and $\alpha_V\beta_3$ is weak. (A,B) Maximum adhesion force (A) and rupture length (B) histograms with representative retraction force profiles (insets) obtained by recording force–distance curves in PBS between Fg-modified AFM tips and $\alpha_V\beta_3$ immobilized on solid substrates. Data from 3 different tips (3072 curves).

3C) or Fg-treated ClfA$^{(-)}$ cells (Figure 3D). Second, the high specificity of the bond was demonstrated by showing a strong inhibition of adhesion with the following blocking agents: anti-$\alpha_V\beta_3$ antibody (LM609), RGD, and cilengitide (adhesion frequency of 3%, 5%, and 6%; adhesion force of 98 ± 36 pN, 147 ± 73 pN, and 82 ± 30 pN, respectively; Figure 3E–G; for data on more cells see Figure 5A). Third, we found that addition of a short γ-chain peptide strongly blocked the adhesion of Fg-treated ClfA$^{(+)}$ cells (frequency of 6%, adhesion force of 103 ± 47 pN, Figure 3H; for data on more cells see Figure 5A), thus confirming the importance of the Fg-ClfA DLL bond in the interaction. Note that Fg induces conformational changes in FnBPs resulting in buried plasminogen-binding domains to be exposed, thereby promoting strong interactions with plasminogen.[28] Our γ-chain peptide experiment allows us to exclude such a mechanism in which structural changes in ClfA would favor strong direct binding to integrins. Collectively, these results lead us to believe that the ~800 pN force represents the rupture of a strong Fg-dependent bridge between ClfA and $\alpha_V\beta_3$, whereas the ~1600 pN force sometime observed would result from the simultaneous rupture of two ClfA-Fg-$\alpha_V\beta_3$ complexes. The ~250 pN force represents another weak specific ClfA-Fg-$\alpha_V\beta_3$ bond. Both ~250 and ~800 pN bonds are highly specific (see controls above) and involve RGD sequences as they were inhibited by soluble RGD and cilengitide. This implies that in our force experiments the two γ-chain-derived non-RGD peptides[20] GWTVFQKRLDGSV$^{190-202}$ and GVYYQGGTYSKAS$^{346-358}$ only contribute modestly to $\alpha_V\beta_3$ binding. These observations suggest a two-site mechanism in which, besides the rather weak RGD$^{572-574}$ binding site, there is a much stronger RGD site located in another domain of Fg. Although in the folded state this site is buried, it may become exposed under mechanical force.

As membrane proteins from mammalian cells are easily extracted from the membrane under high forces, one may wonder whether our high forces are biologically relevant. First, it is likely that in vivo clustering of integrins will increase the strength and avidity of the interaction. Second, other binding mechanisms via other adhesins and ligands are likely to contribute to the overall adhesion. Third, the stretching geometry clearly differs between in vitro and in vivo conditions, and as the pulling geometry impacts binding forces this may explain why integrins can sustain high forces in vivo.

Mechanostability of the ClfA-Fg-$\alpha_V\beta_3$ Complex. To further dissect the molecular details of the mechanostability of the ClfA-Fg-$\alpha_V\beta_3$ bond, we measured the forces between AFM tips functionalized with $\alpha_V\beta_3$ and *S. aureus* ClfA$^{(+)}$ cells pretreated with soluble Fg (Figure 4). Adhesion forces were frequently detected (~37% mean on 3 cells) and showed 2 maxima at 258 ± 67 pN and 713 ± 140 pN (Gaussian fits; n = 1110 adhesive curves from 3 cells, Figure 4A,B; for data on more cells see Figure 5B). These low and high forces are very similar to those observed with whole cells (Figure 3) and were abrogated when using native, untreated ClfA$^{(+)}$ cells (Figure 4C), or Fg-treated ClfA$^{(-)}$ cells (Figure 4D), implying again that they represent the signature of the Fg bridging interaction between ClfA and $\alpha_V\beta_3$.

Interestingly, sawtooth patterns were observed in a number of curves (~15% of all adhesive curves), each peak corresponding to the force-induced unfolding of an individual protein domain. We argue that these multipeak signatures originate from the unusual elasticity and extensibility of the Fg molecule, particularly the C-terminal γ-chain nodules and, to some extent, the α-helical coiled-coil connectors.[29] As unfolding of the γ-nodules (2 × 411 residues) largely contributes to protein unfolding, we expect protein extensions of ~300 nm, which is what we observed, 300 ± 86 nm (n = 1110; 3 cells). A few ~600 nm extensions were observed, likely to be associated with dimers, as these are known to form at solid–liquid interfaces.[30] Earlier simulation and AFM experiments[29] have revealed that under force, 10–15 nm extension of the α-helical coiled-coil connectors occurs, followed by sequential unraveling of the compact globular structural domains in the γ-nodules, leading to protein extensions in the 25–33 nm range. Consistent with this, ~15% of adhesive curves displayed multiple small peaks of 88 ± 22 pN separated by 12 ± 2 nm, followed by larger peaks of 138 ± 37 pN separated by 23 ± 2 nm (Figure 4E,F). The number of peaks (~5–8 for both low and high forces) is consistent with those expected for Fg monomers and dimers,[29] suggesting that dimers are also involved in the bridging interaction.

We reasoned that the weakest side of the ClfA-Fg-$\alpha_V\beta_3$ complex should be the Fg-$\alpha_V\beta_3$ bond, as the Fg-ClfA bond is very strong (~1500 pN).[22] Intriguingly, we found that the

DOI: 10.1021/acs.nanolett.9b03080
Nano Lett. 2019, 19, 7400–7410

strength of the Fg-$\alpha_V\beta_3$ bond (74 ± 13 pN; Figure 6) is in the range of that of classical RGD-integrin binding strengths (~100 pN range),[31−34] thus much lower than the strength of the three-component complex (~800 pN). This unexpected behavior leads us to believe that under mechanical force, extension of Fg leads to the exposure of a strong cryptic RGD site. Analysis of the primary structures of the mechanically sensitive domains, the γ-chain nodules, and the α-helical coiled-coils[29] indeed reveals a buried RGD^{95-97} site in the latter whereas the γ-chain nodules lack any RGD sequence. These observations argue in favor of a two-site mechanism in which, besides the rather weak $RGD^{572-574}$ binding site, there is a much stronger site located in the Aα chain, RGD^{95-97}. Supporting this mechanical model, single-molecule stretching experiments have shown that mechanical force leads to the unfolding of the C-terminal γ-chain nodules and to the extension of the α-helical coiled-coil connectors.[29]

In conclusion, sepsis is a life-threatening condition resulting from the presence of harmful bacteria, especially *S. aureus*,[35] in the blood that can lead to tissue damage, organ failure, and death.[4] The disease initially occurs when the pathogens access the bloodstream and bind to the endothelium, thereby impairing vascular functions with consequent vasodilation, increased vascular permeability and edema, cardiac depression, and alteration of the coagulation cascade. The success of *S. aureus* as an etiological agent of sepsis is largely due to the expression of adhesins, particularly clumping factor A (ClfA), a key virulence factor in bloodstream infections.[36,37] ClfA is involved in binding to $\alpha_V\beta_3$, the latter being upregulated in sepsis patients.[38] Understanding the mechanism by which ClfA binds to endothelial cells is thus of both biological and medical relevance.

We have identified a novel stress-dependent binding mechanism in which the simultaneous binding of Fg to ClfA and $\alpha_V\beta_3$ leads to an extremely strong three-component interaction. Such a mechanically stable bridge was unexpected and surprising as the ClfA-Fg-$\alpha_V\beta_3$ interaction is about ten times stronger than the Fg-$\alpha_V\beta_3$ bond. Adhesion force signatures feature periodic peaks that result from the unfolding of the Fg γ chain nodules and extension of α-helical coiled-coils, suggesting that domain folding/unfolding plays an important role in the mechanostability of the bond. We propose that the ClfA-Fg complex binds to $\alpha_V\beta_3$ by means of two distinct RGD sites, which adhesion strength is activated by mechanical tension. At low stress, the $RGD^{572-574}$ sequences in the Aα chains mediate weak binding to $\alpha_V\beta_3$. At high stress, exposure of the RGD^{95-97} residues favor strong binding to the integrin. This mechanoregulated adhesion mechanism contributes to the growing body of evidence showing that mechanical forces play an essential role in regulating staphylococcal adhesion.[11,39,40]

To understand the physics of force activation in bacterial adhesion, one must appreciate the difference between affinity values measured at equilibrium versus binding strengths probed under force, out of equilibrium. Under tensile loading, conformational changes in a protein−ligand complex may lead to strong binding forces even if the affinity is low. In previous studies, the binding sites and affinity of Fg for $\alpha_V\beta_3$ were determined in the absence of shear stress with full-length Fg or isolated chains and in the presence of inhibitory synthetic peptides.[18,20,27] As during bloodstream infection, bacteria, endothelial cells, and ECM matrix are subjected to considerable shear, we argue that adhesion parameters should be probed under physical stress, as in flow chambers (population) and AFM (single-molecule) experiments, rather than at equilibrium.

As ligand binding by integrins triggers intracellular signaling cascades that strengthen cell adhesion, it is possible that the mechanically strong bridge contributes to signaling. It has been shown that the signaling-and migration-incapable $\alpha_V\beta_3$-TMD mutant TMD-GpA (transmembrane domain of glycophorin A) features the characteristics of a primed integrin state, which is of low basal affinity in the absence of force but forms strong bonds (~200 pN) in the presence of force.[41] Being ideally suited to function as a force sensor, TMDGpA may thus mimic a force-activatable signaling intermediate with low basal affinity. Our findings parallel these results, providing a possible molecular basis for understanding the high mechanostability of the ClfA-Fg-$\alpha_V\beta_3$ ternary complex during *S. aureus* adhesion to endothelium.

Our study could have important implications for the design of new therapeutics against *S. aureus*. Blocking $\alpha_V\beta_3$ with cilengitide resulted in a significant reduction in the endothelial cell permeability induced by *S. aureus* and stabilization of the VE-cadherin contacts, suggesting that preventing the ClfA-$\alpha_V\beta_3$ interaction with cilengitide arrests the signal that leads to apoptosis and the subsequent reduction in VE-cadherin expression, thus reducing the possibility of an increase in vascular permeability. This supports recent findings suggesting that cilengitide could be potentially used as an antiadhesion drug, together with antibiotics, to fight sepsis.[7]

Methods. *Bacterial Strains and Growth Conditions.* *S. aureus* $ClfA^{(-)}$ is a *S. aureus* SH1000 *clfA clfB fnbA fnbB* strain defective in both clumping factors A and B and fibronectin-binding proteins A and B[42] whereas *S. aureus* $ClfA^{(+)}$ is SH1000 *clfA clfB fnbA fnbB* transformed with the plasmid pCU1::clfA.[43] All strains were grown in trypticase soy agar or trypticase soy broth with shaking at 200 rpm at 37 °C to stationary phase. *S.aureus* $ClfA^{(+)}$ was grown with 10 $\mu g \cdot mL^{-1}$ chloramphenicol. For AFM experiments, cells were harvested by centrifugation at 3000×*g* for 5 min and washed twice with PBS. For some experiments, bacteria were preincubated for 60 min with 0.1 $mg.mL^{-1}$ of soluble fibrinogen (sigma) or the C-terminal segment of the Fg γ-chain (0.2 $mg.mL^{-1}$).

Endothelial Cell Culture. Endothelial cells (HUVEC) were cultured in endothelial basal medium (EBM) supplemented with 2% fetal bovine serum (FBS), 0.4% bovine brain extract, 0.1% human epidermal grow factor, 0.1% hydrocortisone, 0.1% ascorbic acid, and 0.1% gentamicin/amphotericin at 37 °C in 5% CO_2 according to manufacturer's instructions (Lonza). Cultured cells were dissociated from plastic flasks using trypsin-EDTA solution (Lonza) and approximatively 5×10^5 cells (in 1 mL EBM medium without antibiotics) were seeded into 24-well plates (Nunc) and allowed to attach for 48 h at 37° in 5% CO_2. Cell confluency was verified by inverted light microscopy.

Bacterial Adherence to $\alpha_V\beta_3$-Coated Microtiter Wells. Microtiter wells were coated overnight at 4 °C with 250 ng/well $\alpha_v\beta_3$ in 0.1 M sodium carbonate, pH 9.5. The plates were washed with PBS containing 0.5% (v/v) Tween 20 (PBST). To block additional protein binding sites, the wells were treated for 1 h at 22 °C with 2% (v/v) bovine serum albumin (BSA) in PBS. Wells were then preincubated for 1 h with 1 μg of Fg in the presence/absence of 10 μg Fg γ chain (residues 400−411) in PBS containing 1 mM $MgCl_2$ and incubated in the same buffer for 1 h with 5×10^7 cells of *S. aureus* $ClfA^{(+)}$ or

DOI: 10.1021/acs.nanolett.9b03080
Nano Lett. 2019, 19, 7400−7410

ClfA$^{(-)}$. To evaluate the effect of RGD or RGE peptides (Sigma-Aldrich, St. Louis, Missouri, U.S.A.) on adhesion, the peptides were added 15 min prior to addition of the bacterial cells. After being washed with PBS containing 1 mM $MgCl_2$, plates were incubated for 1 h with horseradish peroxidase (HRP)-conjugated mouse IgG diluted 1:1000. After further washing, *o*-phenylendiamine dihydochloride was added to the wells, and the absorbance at 490 nm was determined using an ELISA plate reader.

Bacterial Attachment to Endothelial Cell Monolayers. Confluent monolayers of HUVEC cells in microtiter plates were washed with PBS and incubated with 1×10^7 of *S. aureus* ClfA$^{(+)}$ or ClfA$^{(-)}$ bacteria in EMB medium containing 10% FBS and without antibiotics for 90 min at 37 °C in 5% CO_2. The effect of Fg on bacterial adhesion to monolayers was tested by pretreating the cells with 10 $\mu g \cdot mL^{-1}$ of the protein 1 h prior to addition of the bacteria. To evaluate the effect of synthetic peptides on adhesion, monolayers pretreated with Fg were incubated with ClfA$^{(+)}$ in the presence of RGD or RGE peptides. After being washed with PBS, plates were incubated with horseradish peroxidase-conjugated mouse IgG diluted 1:1000. After further washing, *o*-phenylendiamine dihydochloride was added to the wells, and the absorbance at 490 nm measured as reported above. Alternatively, bacterial attachment was determined by counting colony forming units (CFU) associated with the monolayers. To this end, HUVEC monolayers in 24-well plates were incubated with 5×10^7 ClfA$^{(+)}$ in the presence/absence of 10 μg/mL Fg, washed with PBS and finally added with 500 μL 0.5% Triton X-100 in PBS for 10 min at 37 °C in 5% CO_2. To ensure the cells fully lysed and released all internalized bacteria, suspensions were agitated by pipetting. CFU were determined by serial dilution of endothelial cell lysates and plating onto BHI agar plates overnight at 37 °C.

Functionalization of Substrates and Cantilevers with Integrins. Gold-coated glass coverslips and cantilevers (OMCL-TR4, Olympus Ltd., Tokyo, Japan; nominal spring constant ~0.02 $N.m^{-1}$) were immersed overnight in an ethanol solution containing 1 mM of 10% 16-mercaptododecahexanoic acid/90% 1-mercapto-1-undecanol (Sigma), rinsed with ethanol and dried with N_2. Substrates and cantilevers were then immersed for 30 min into a solution containing 10 mg·mL^{-1} *N*-hydroxysuccinimide (NHS) and 25 mg·mL^{-1} 1-ethyl-3-(3- dimethylaminopropyl)-carbodiimide (EDC) (Sigma), rinsed with ultrapure water (ELGA LabWater), incubated with 0.1 mg·mL^{-1} of integrin $\alpha_V\beta_3$ (Merck) for 1 h, rinsed further with PBS buffer, and then immediately used without dewetting.

Bacterial Adhesion to Integrin-Coated Surfaces. Adhesion of *S.aureus* bacteria was assessed on integrin $\alpha_V\beta_3$-functionalized surfaces in static and dynamic conditions. For static experiments, bacterial suspensions in PBS were incubated with $\alpha_V\beta_3$ surfaces for 2 h at 37 °C, gently rinsed with PBS, and imaged using an optical microscope Zeiss Axio Observer Z1 and a Hamamatsu camera C10600. For flow experiments, bacterial suspensions were flowed over integrin $\alpha_V\beta_3$ surfaces for 2 min using a fluidic chamber,[44] using a peristaltic pump (Miniplus, Gilson). Two different flow rates were tested, 2 and 20 mL·min^{-1}, corresponding to shear rates of 12 and 120 s^{-1}, respectively. Loosely attached bacteria were removed by flowing PBS during 2 min using the corresponding flow rate. Adhering bacteria were imaged using an inverted microscope (Leica DM16000) and counted using the ImageJ image analysis software (NIH Image).

Single-Cell Force Spectroscopy. Colloidal probes were obtained by attaching single silica microsphere (6.1 μm diameter, Bangs laboratories) with a thin layer of UV-curable glue (NOA 63, Norland Edmund Optics) on triangular shaped tip-less cantilevers (NP-O10, Bruker) using a Nanowizard IV AFM (JPK Instrument, Berlin, Germany). Cantilevers were then immersed for 1 h in Tris-buffered saline (TBS; Tris, 50 mM; NaCl, 150 mM; pH 8.5) containing 4 mg·mL^{-1} dopamine hydrochloride (Sigma-Aldrich), rinsed in TBS, and used directly for cell probe preparation. The nominal spring constant of the colloidal probe was determined by the thermal noise method. Fifty microliters of a suspension of about 1×10^6 cells were transferred into a glass Petri dish containing $\alpha_v\beta_3$-coated substrates in PBS. The colloidal probe was brought into contact with a single bacterium and the cell probe was then positioned over the integrin $\alpha_v\beta_3$-substrate without dewetting. Cell probes were used to measure interaction forces on integrin $\alpha_v\beta_3$-surfaces at room temperature by recording multiple forces curves (16 × 16) on different spots with a maximum applied force of 250 pN, and approach and retraction speeds of 1000 nm·s^{-1}. Histograms were generated by considering for every curve the force and the distance of the last rupture event. For some blocking experiments, we used commercially available RGDFV peptide (Sigma-Aldrich), cilengitide (Sigma), or anti$\alpha v\beta 3$ antibody LM 609 (Abcam). Histograms were generated by considering for every curve the force and the distance of the last rupture event.

Single-Molecule Force Spectroscopy. For SMFS experiments on bacteria, cantilevers were prepared as described above and the cells were immobilized on polystyrene substrates. Measurements were performed at room temperature in PBS with a NanoWizard IV AFM (JPK Instruments). Multiple (32 × 32) force−distance curves were recorded on areas of 500 × 500 nm^2 with an applied force of 250 pN, a constant approach, and retraction speed of 1000 nm·s^{-1}. For SMFS experiments on model surfaces, substrates and cantilevers were prepared as described above and multiple (32 × 32) force−distance curves were recorded on areas of 5 by 5 μm.[2] Histograms were generated by considering, for every curve, the force and the distance of the last rupture event. The spring constants of the cantilevers were measured by the thermal noise method. Data were analyzed with the data processing software from JPK Instruments (Berlin, Germany).

AUTHOR INFORMATION

Corresponding Authors

*(Y.D.) E-mail: yves.dufrene@uclouvain.be.
*(G.P.) E-mail: giampiero.pietrocola@unipv.it.

ORCID

Giampiero Pietrocola: 0000-0002-7069-8155
Yves F. Dufrêne: 0000-0002-7289-4248

Author Contributions

F.V., P.S., G.P., and Y.F.D. designed the experiments, analyzed the data, and wrote the article. F.V. collected the data.

Notes

The authors declare no competing financial interest.

DOI: 10.1021/acs.nanolett.9b03080
Nano Lett. 2019, 19, 7400−7410

■ ACKNOWLEDGMENTS

Work at the Université catholique de Louvain was supported by the European Research Council (ERC) under the European Union's Horizon 2020 research and innovation programme (Grant Agreement 693630), the FNRS-WELBIO (Grant WELBIO-CR-2015A-05), the National Fund for Scientific Research (FNRS), and the Research Department of the Communauté française de Belgique (Concerted Research Action). Funding by the Fondazione CARIPLO (Grant Vaccines 2009-3546) to P.S. is acknowledged. Y.F.D. is Research Director at the FNRS. We thank Joan Geoghegan and Timothy Foster for fruitful discussion and for providing bacterial strains and Audrey Leprince and Jacques Mahillon for help with flow experiments.

■ REFERENCES

(1) Byrd, A. L.; Belkaid, Y.; Segre, J. A. The human skin microbiome. *Nat. Rev. Microbiol.* **2018**, *16*, 143−155.
(2) Parlet, C. P.; Brown, M. M.; Horswill, A. R. Commensal staphylococci influence *Staphylococcus aureus* skin colonization and disease. *Trends Microbiol.* **2019**, *27*, 497−507.
(3) Thomer, L.; Schneewind, O.; Missiakas, D. Pathogenesis of *Staphylococcus aureus* bloodstream infections. *Annu. Rev. Pathol.: Mech. Dis.* **2016**, *11*, 343−364.
(4) Angus, D. C.; van der Poll, T. Severe sepsis and septic shock. *N. Engl. J. Med.* **2013**, *369*, 840−851.
(5) Foster, T. J.; Geoghegan, J. A.; Ganesh, V. K.; Höök, M. Adhesion, invasion and evasion: The many functions of the surface proteins of *Staphylococcus aureus*. *Nat. Rev. Microbiol.* **2014**, *12*, 49−62.
(6) Claes, J.; Ditkowski, B.; Liesenborghs, L.; Veloso, T. R.; Entenza, J. M.; Moreillon, P.; Vanassche, T.; Verhamme, P.; Hoylaerts, M. F.; Heying, R. Assessment of the dual role of clumping factor A in *S. aureus* adhesion to endothelium in absence and presence of plasma. *Thromb. Haemostasis* **2018**, *118*, 1230−1241.
(7) McDonnell, C. J.; Garciarena, C. D.; Watkin, R. L.; McHale, T. M.; McLoughlin, A.; Claes, J.; Verhamme, P.; Cummins, P. M.; Kerrigan, S. W. Inhibition of major integrin $\alpha_V\beta_3$ reduces *Staphylococcus aureus* attachment to sheared human endothelial cells. *J. Thromb. Haemostasis* **2016**, *14*, 2536−2547.
(8) Ganesh, V. K.; Rivera, J. J.; Smeds, E.; Ko, Y.-P.; Bowden, M. G.; Wann, E. R.; Gurusiddappa, S.; Fitzgerald, J. R.; Höök, M. A structural model of the *Staphylococcus aureus* ClfA−fibrinogen interaction opens new avenues for the design of anti-staphylococcal therapeutics. *PLoS Pathog.* **2008**, *4*, No. e1000226.
(9) Ponnuraj, K.; Bowden, M. G.; Davis, S.; Gurusiddappa, S.; Moore, D.; Choe, D.; Xu, Y.; Hook, M.; Narayana, S. V. L. A "Dock, Lock, and Latch" structural model for a staphylococcal adhesin binding to fibrinogen. *Cell* **2003**, *115*, 217−228.
(10) Herman, P.; El-Kirat-Chatel, S.; Beaussart, A.; Geoghegan, J. A.; Foster, T. J.; Dufrêne, Y. F. The binding force of the staphylococcal adhesin SdrG is remarkably strong. *Mol. Microbiol.* **2014**, *93*, 356−368.
(11) Milles, L. F.; Schulten, K.; Gaub, H. E.; Bernardi, R. C. Molecular mechanism of extreme mechanostability in a pathogen adhesin. *Science* **2018**, *359*, 1527−1533.
(12) Ganesh, V. K.; Liang, X.; Geoghegan, J. A.; Cohen, A. L. V.; Venugopalan, N.; Foster, T. J.; Hook, M. Lessons from the crystal structure of the *S. aureus* surface protein clumping factor A in complex with Tefibazumab, an inhibiting monoclonal antibody. *EBioMedicine* **2016**, *13*, 328−338.
(13) Hynes, R. O. Integrins: Bidirectional, allosteric signaling machines. *Cell* **2002**, *110*, 673−687.
(14) Barczyk, M.; Carracedo, S.; Gullberg, D. *Cell Tissue Res.* **2010**, *339*, 269−280.
(15) Eliceiri, B. P.; Cheresh, D. A. The role of α_V integrins during angiogenesis: Insights into potential mechanisms of action and clinical development. *J. Clin. Invest.* **1999**, *103*, 1227−1230.
(16) Plow, E. F.; Haas, T. A.; Zhang, L.; Loftus, J.; Smith, J. W. Ligand binding to integrins. *J. Biol. Chem.* **2000**, *275*, 21785−21788.
(17) Xiong, J.-P.; Stehle, T.; Diefenbach, B.; Zhang, R.; Dunker, R.; Scott, D. L.; Joachimiak, A.; Goodman, S. L.; Arnaout, M. A. Crystal structure of the extracellular segment of integrin $\alpha_V\beta_3$. *Science* **2001**, *294*, 339−345.
(18) Smith, J. W.; Ruggeri, Z. M.; Kunicki, T. J.; Cheresh, D. A. Interaction of integrins alpha V beta 3 and glycoprotein IIb-IIIa with fibrinogen. Differential peptide recognition accounts for distinct binding sites. *J. Biol. Chem.* **1990**, *265*, 12267−12271.
(19) Cheresh, D. A.; Berliner, S. A.; Vicente, V.; Ruggeri, Z. M. Recognition of distinct adhesive sites on fibrinogen by related integrins on platelets and endothelial cells. *Cell* **1989**, *58*, 945−953.
(20) Yokoyama, K.; Erickson, H. P.; Ikeda, Y.; Takada, Y. Identification of amino acid sequences in fibrinogen γ-chain and tenascin C C-terminal domains critical for binding to integrin $\alpha_V\beta_3$. *J. Biol. Chem.* **2000**, *275*, 16891−16898.
(21) Xiao, J.; Dufrêne, Y. F. Optical and force nanoscopy in microbiology. *Nat. Microbiol.* **2016**, *1*, 16186.
(22) Herman-Bausier, P.; Labate, C.; Towell, A. M.; Derclaye, S.; Geoghegan, J. A.; Dufrêne, Y. F. *Staphylococcus aureus* clumping factor A is a force-sensitive molecular switch that activates bacterial adhesion. *Proc. Natl. Acad. Sci. U. S. A.* **2018**, *115*, 5564−5569.
(23) Borst, A. J.; James, Z. M.; Zagotta, W. N.; Ginsberg, M.; Rey, F. A.; DiMaio, F.; Backovic, M.; Veesler, D. The therapeutic antibody LM609 selectively inhibits ligand binding to human $\alpha_V\beta_3$ integrin via steric hindrance. *Structure* **2017**, *25*, 1732−1739.
(24) Kroll, M. H.; Hellums, J. D.; McIntire, L. V.; Schafer, A. I.; Moake, J. L. Platelets and shear stress. *Blood* **1996**, *88*, 1525−1541.
(25) Kapp, T. G.; Rechenmacher, F.; Neubauer, S.; Maltsev, O. V.; Cavalcanti-Adam, E. A.; Zarka, R.; Reuning, U.; Notni, J.; Wester, H.-J.; Mas-Moruno, C. A comprehensive evaluation of the activity and selectivity profile of ligands for RGD-binding integrins. *Sci. Rep.* **2017**, *7*, 39805.
(26) McDevitt, D.; Francois, P.; Vaudaux, P.; Foster, T. J. Identification of the ligand-binding domain of the surface-located fibrinogen receptor (clumping factor) of *Staphylococcus aureus*. *Mol. Microbiol.* **1995**, *16*, 895−907.
(27) Mcdevitt, D.; Nanavaty, T.; House-Pompeo, K.; Bell, E.; Turner, N.; Mcintire, L.; Foster, T.; HööK, M. Characterization of the interaction between the *Staphylococcus aureus* clumping factor (ClfA) and fibrinogen. *Eur. J. Biochem.* **1997**, *247*, 416−424.
(28) Herman-Bausier, P.; Pietrocola, G.; Foster, T. J.; Speziale, P.; Dufrêne, Y. F. Fibrinogen activates the capture of human plasminogen by staphylococcal fibronectin-binding proteins. *mBio* **2017**, *8*, e01067−17.
(29) Zhmurov, A.; Brown, A. E. X.; Litvinov, R. I.; Dima, R. I.; Weisel, J. W.; Barsegov, V. Mechanism of fibrin (ogen) forced unfolding. *Structure* **2011**, *19*, 1615−1624.
(30) Kastantin, M.; Langdon, B. B.; Chang, E. L.; Schwartz, D. K. Single-Molecule resolution of interfacial fibrinogen behavior: effects of oligomer populations and surface chemistry. *J. Am. Chem. Soc.* **2011**, *133*, 4975−4983.
(31) Li, F.; Redick, S. D.; Erickson, H. P.; Moy, V. T. Force measurements of the $\alpha_v\beta_1$ integrin−fibronectin interaction. *Biophys. J.* **2003**, *84*, 1252−1262.
(32) Müller, D. J.; Helenius, J.; Alsteens, D.; Dufrêne, Y. F. Force probing surfaces of living cells to molecular resolution. *Nat. Chem. Biol.* **2009**, *5*, 383−390.
(33) Bharadwaj, M.; Strohmeyer, N.; Colo, G. P.; Helenius, J.; Beerenwinkel, N.; Schiller, H. B.; Fässler, R.; Müller, D. J. AV-Class Integrins exert dual roles on $\alpha_v\beta_1$ integrins to strengthen adhesion to fibronectin. *Nat. Commun.* **2017**, *8*, 14348.
(34) Strohmeyer, N.; Bharadwaj, M.; Costell, M.; Fässler, R.; Müller, D. J. fibronectin-bound $\alpha_v\beta_1$ integrins sense load and signal to

DOI: 10.1021/acs.nanolett.9b03080
Nano Lett. 2019, 19, 7400−7410

reinforce adhesion in less than a second. *Nat. Mater.* **2017**, *16*, 1262−1270.
(35) Vincent, J.-L.; Rello, J.; Marshall, J.; Silva, E.; Anzueto, A.; Martin, C. D.; Moreno, R.; Lipman, J.; Gomersall, C.; Sakr, Y. International study of the prevalence and outcomes of infection in intensive care units. *JAMA* **2009**, *302*, 2323−2329.
(36) Flick, M. J.; Du, X.; Prasad, J. M.; Raghu, H.; Palumbo, J. S.; Smeds, E.; Höök, M.; Degen, J. L. Genetic elimination of the binding motif on fibrinogen for the *S. aureus* virulence factor clfa improves host survival in septicemia. *Blood* **2013**, *121*, 1783−1794.
(37) Tkaczyk, C.; Kasturirangan, S.; Minola, A.; Jones-Nelson, O.; Gunter, V.; Shi, Y. Y.; Rosenthal, K.; Aleti, V.; Semenova, E.; Warrener, P.; et al. Multimechanistic monoclonal antibodies (mAbs) targeting *Staphylococcus aureus* alpha-toxin and clumping factor a: activity and efficacy comparisons of a mAb combination and an engineered bispecific antibody approach. *Antimicrob. Agents Chemother.* **2017**, *61*, e00629−17.
(38) Singh, B.; Janardhan, K. S.; Kanthan, R. Expression of Angiostatin, integrin $\alpha_v\beta_3$, and vitronectin in human lungs in sepsis. *Exp. Lung Res.* **2005**, *31*, 771−782.
(39) Herman-Bausier, P.; Dufrêne, Y. F. Force matters in hospital-acquired infections. *Science* **2018**, *359*, 1464−1465.
(40) Geoghegan, J. A.; Dufrêne, Y. F. Mechanomicrobiology: How mechanical forces activate *Staphylococcus aureus* adhesion. *Trends Microbiol.* **2018**, *26*, 645−648.
(41) Müller, M. A.; Opfer, J.; Brunie, L.; Volkhardt, L. A.; Sinner, E.-K.; Boettiger, D.; Bochen, A.; Kessler, H.; Gottschalk, K.-E.; Reuning, U. The glycophorin a transmembrane sequence within integrin $\alpha_v\beta_3$ creates a non-signaling integrin with low basal affinity that is strongly adhesive under force. *J. Mol. Biol.* **2013**, *425*, 2988−3006.
(42) O'Neill, E.; Pozzi, C.; Houston, P.; Humphreys, H.; Robinson, D. A.; Loughman, A.; Foster, T. J.; O'Gara, J. P. A Novel *Staphylococcus aureus* biofilm phenotype mediated by the fibronectin-binding proteins, FnBPA and FnBPB. *J. Bacteriol.* **2008**, *190*, 3835−3850.
(43) McCormack, N.; Foster, T. J.; Geoghegan, J. A. A Short sequence within subdomain N1 of region A of the *Staphylococcus aureus* MSCRAMM clumping factor A is required for export and surface display. *Microbiology* **2014**, *160*, 659−670.
(44) Vanzieleghem, T.; Couniot, N.; Herman-Bausier, P.; Flandre, D.; Dufrêne, Y. F.; Mahillon, J. Role of ionic strength in staphylococcal cell aggregation. *Langmuir* **2016**, *32*, 7277−7283.

DOI: 10.1021/acs.nanolett.9b03080
Nano Lett. 2019, 19, 7400−7410